British Journal of Pharmacology

DOI:10.1111/bph.12993
www.brjpharmacol.org

RESEARCH PAPER

FM19G11 reverses endothelial dysfunction in rat and human arteries through stimulation of the PI3K/Akt/eNOS pathway, independently of mTOR/HIF-1α activation

Correspondence
José M Sánchez-Puelles, Molecular Pharmacology Group, Cellular and Molecular Medicine Department, Centro de Investigaciones Biológicas, Consejo Superior de Investigaciones Científicas, c/Ramiro de Maeztu 9, 28040 Madrid, Spain. E-mail: jm.spuelles@csic.es

*Both authors contributed equally.

Received
14 July 2014
Revised
23 October 2014
Accepted
27 October 2014

M El Assar[1]*, J M Sánchez-Puelles[1,2]*, I Royo[2], E López-Hernández[2], A Sánchez-Ferrer[1], J L Aceña[3], L Rodríguez-Mañas[1,4] and J Angulo[5]

[1]*Fundación para la Investigación Biomédica del Hospital Universitario de Getafe, Getafe, Madrid, Spain,* [2]*Molecular Pharmacology Group, Cellular and Molecular Medicine Department, Centro de Investigaciones Biológicas, Consejo Superior de Investigaciones Científicas, Madrid, Spain,* [3]*Departamento de Química Orgánica Facultad de Química, Universidad del País Vasco UPV/EHU, San Sebastián, Spain,* [4]*Servicio de Geriatría, Hospital Universitario de Getafe, Getafe, Madrid, Spain, and* [5]*Instituto Ramón y Cajal de Investigación Sanitaria (IRYCIS), Hospital Universitario Ramón y Cajal, Madrid, Spain*

BACKGROUND AND PURPOSE

FM19G11 up-regulates mammalian target of rapamycin (mTOR)/hypoxia inducible factor-1α (HIF-1α) and PI3K/Akt pathways, which are involved in endothelial function. We evaluated the effects of FM19G11 on defective endothelial vasodilatation in arteries from rats and humans and investigated the mechanisms involved.

EXPERIMENTAL APPROACH

Effects of chronic *in vivo* administration of FM19G11 on aortic endothelial vasodilatation were evaluated together with *ex vivo* treatment in aortic and mesenteric arteries from control and insulin-resistant rats (IRR). Its effects on vasodilator responses of penile arteries (HPRAs) and corpus cavernosum (HCC) from men with vasculogenic erectile dysfunction (ED) (model of human endothelial dysfunction) were also evaluated. Vascular expression of phosphorylated-endothelial NOS (p-eNOS), phosphorylated-Akt (p-Akt) and HIF-1α was determined by immunodetection and cGMP by ELISA.

KEY RESULTS

Chronic administration of FM19G11 reversed the impaired endothelial vasodilatation in IRR. *Ex vivo* treatment with FM19G11 also significantly improved endothelium-dependent vasodilatation in aorta and mesenteric arteries from IRR. These effects were accompanied by the restoration of p-eNOS and cGMP levels in IRR aorta and were prevented by either NOS or PI3K inhibition. p-Akt and p-eNOS contents were increased by FM19G11 in aortic endothelium of IRR. FM19G11-induced restoration of endothelial vasodilatation was unaffected by mTOR/HIF-1α inhibitors. FM19G11 also restored endothelial vasodilatation in HPRA and HCC from ED patients.

CONCLUSIONS AND IMPLICATIONS

Stimulation of the PI3K/Akt/eNOS pathway by FM19G11 alleviates impaired NO-mediated endothelial vasodilatation in rat and human arteries independently of mTOR/HIF-1α activation. This pharmacological strategy could be beneficial for managing pathological conditions associated with endothelial dysfunction, such as ED.

Abbreviations

CR, control rats; ED, erectile dysfunction; eNOS, endothelial NOS; HCC, human corpus cavernosum; HIF-1α, hypoxia inducible factor-1α; HPRA, human penile resistance arteries; IRR, insulin-resistant rats; L-NAME, N^G-nitro-L-arginine methyl ester; mTOR, mammalian target of rapamycin; p-eNOS, phosphorylated eNOS; p-Akt, phosphorylated-Akt; SNP, sodium nitroprusside

Tables of Links

TARGETS
Akt (PKB)
ATR serine/threonine kinase
Endothelial (e) NOS
mTOR
PI3K
Soluble guanylyl cyclase (sGC)

LIGANDS	
ACh	Noradrenaline (NA)
Bradykinin	Phenylephrine
cGMP	Rapamycin
Insulin	Thrombin
L-NAME	Wortmannin
Nitric oxide (NO)	

These Tables list key protein targets and ligands in this article which are hyperlinked to corresponding entries in http://www.guidetopharmacology.org, the common portal for data from the IUPHAR/BPS Guide to PHARMACOLOGY (Pawson *et al.*, 2014) and are permanently archived in the Concise Guide to PHARMACOLOGY 2013/14 (Alexander *et al.*, 2013).

Introduction

Endothelial dysfunction is a key process in the pathogenesis of cardiovascular disease. It precedes the disease's clinical manifestations and predicts future cardiovascular events (Green *et al.*, 2011). Situations increasing the risk of cardiovascular disease, such as diabetes, hypertension and ageing, are clearly associated with the presence of endothelial dysfunction. Therapeutic strategies targeted at preserving or restoring endothelial function are key to the prevention of cardiovascular disease. NO participates in many functions of the endothelium and is a key mediator of endothelium-dependent vasodilatation. In fact, the main risk factors for cardiovascular disease in humans all share the characteristic of defective NO-mediated vasodilatation (Paniagua *et al.*, 2001; Rodríguez-Mañas *et al.*, 2009; Angulo *et al.*, 2010). Thus, restoring NO signalling is a suitable strategy for overcoming endothelial dysfunction and preventing cardiovascular disease.

The enzyme responsible for NO generation from the endothelium is endothelial NOS (eNOS). Its activity is triggered by a rise in intracellular calcium in response to various stimuli (ACh, bradykinin, thrombin, shear stress, etc.) and is also regulated by post-translational mechanisms such as acylation, S-nitrosylation and phosphorylation (Michel and Vanhoutte, 2010). Among these, PI3K/Akt-dependent phosphorylation at Ser^{1177} is an important mechanism for enhancing NO synthesis by eNOS (Fisslthaler *et al.*, 2000; Hisamoto *et al.*, 2001; Symons *et al.*, 2009). Furthermore, defective PI3K/Akt-dependent phosphorylation of eNOS contributes to the impairment of NO-mediated vasodilatation in several pathological conditions, including insulin resistance (Kobayashi *et al.*, 2004; Li *et al.*, 2010; Zhang *et al.*, 2012).

Insulin resistance is a pathological condition defined by a defective action of insulin on target organs, compensated for by increased insulin secretion to maintain circulating glucose concentrations in the normal range. In addition to predicting type 2 diabetes, insulin resistance represents an important risk factor for the development of cardiovascular disease (Hanley *et al.*, 2002; Thacker *et al.*, 2011; Reaven, 2012). This is probably related to the effect of insulin resistance on endothelial function, as humans with this condition have been found to have impaired endothelial vasodilatation in different vascular areas (Lteif *et al.*, 2005; Suzuki *et al.*, 2007; Fujii *et al.*, 2008). In fact, induction of insulin resistance by feeding rats with high fructose results in defective endothelium-dependent relaxation in both macro- and microvessels (Katakam *et al.*, 1999; Shinozaki *et al.*, 1999), providing a well-characterized model of endothelial dysfunction (Tran *et al.*, 2009).

Erectile dysfunction (ED) is an indicator of the existence of several peripheral vasculopathies (Goksu *et al.*, 2014) and even predicts the presence of subclinical coronary artery disease (Jackson, 2013). In fact, ED is actually considered to be an indicator of systemic endothelial dysfunction and a sentinel of silent generalized cardiovascular disease (Gandaglia *et al.*, 2014). Vascular ED in men is indeed associated with defects in endothelium-dependent relaxation in key vascular structures involved in penile erection: penile arteries and corpus cavernosum (Angulo *et al.*, 2010), representing an appropriate model of human endothelial dysfunction.

Hypoxia-inducible transcription factor (HIF) has an important role in angiogenesis and several pathological conditions, including cancer, inflammation and cardiovascular and neurodegenerative diseases (Majmundar *et al.*, 2010; Royo *et al.*, 2011). HIF-1α is thought to mediate cardio- and neuroprotection, in part by reprogramming cell metabolism. Therefore, it is conceivable that HIF-1α therapies could be used to treat vascular and metabolic diseases. There is increasing evidence supporting a role for HIF-1α activity in the neoangiogenic response to tissue ischaemia (Bosch-Marce *et al.*, 2007).

Therapies targeted to overcome the endothelial dysfunction associated with ageing and other cardiovascular risk factors are definitely needed. FM19G11 is a novel compound that modulates the transcriptional activity of HIF-α proteins in hypoxic conditions (Moreno-Manzano *et al.*, 2010), while in normoxia it up-regulates the protein expression of HIF-1α through rapid activation of the transcription factor, mammalian target of rapamycin (mTOR) (Rodríguez-Jiménez *et al.*, 2010; 2012). Mechanistic analysis has also revealed that FM19G11 facilitates glucose availability and metabolism in ependymal stem cells by activating the PI3K/Akt pathway (Rodríguez-Jiménez *et al.*, 2012).

The aim of the present study was to evaluate the ability of FM19G11 to reverse the impairment of endothelium-dependent vasodilatation in insulin-resistant rats (IRRs), and determine the involvement of PI3K/Akt/eNOS and mTOR/HIF-1α pathways in this effect. The validity of this pharmacological strategy to overcome endothelial dysfunction in humans was also evaluated in penile resistance arteries (HPRA) and corpus cavernosum (HCC) from patients with vasculogenic ED.

Methods

Animal model of insulin resistance

Studies were performed in accordance with the Declaration of Helsinki and with the Guide for the Care and Use of Laboratory Animals, as adopted and implemented by National Institutes of Health, and were approved by the local Ethics Committee for Animal Experimentation of the Hospital Universitario de Getafe. All studies involving animals are reported in accordance with the ARRIVE guidelines for reporting experiments involving animals (Kilkenny *et al.*, 2010; McGrath *et al.*, 2010). A total of 90 male Wistar rats (Harlan, Barcelona, Spain) were kept under a 12 h light/dark cycle with free access to food and water. Fructose-fed rats were used as a model of insulin resistance. This is a widely characterized model (Tran *et al.*, 2009) that has been shown to be associated with an impairment of endothelial vasodilatation (Shinozaki *et al.*, 1999). Four- to 5-week-old rats were fed fructose (20%) in drinking water for 8 weeks. Age-matched rats maintained in the same conditions, but with no fructose in their drinking water, were used as controls (non-insulin resistant). IRRs continuing on high-fructose diet were treated i.p. (1 mL·kg^{-1}) with FM19G11 (10 mg·kg^{-1}·day^{-1}) or vehicle (25% DMSO) for 7 days. This duration of treatment was chosen based on previously reported functional benefits in spinal cord injury regeneration in rats after 1 week of FM19G11 administration (Rodríguez-Jiménez *et al.*, 2012). Then, rats were killed and aortae and mesenteric arteries were obtained for vascular reactivity experiments. Rats were deprived of food overnight before death and serum was obtained for determination of glucose and insulin concentrations.

Serum glucose and insulin concentrations

Circulating levels of insulin were determined in rat serum by ELISA following the manufacturer's instructions (Mercodia AB, Uppsala, Sweden; cat. # 10-1250-01). Serum glucose concentrations were determined by a colorimetric commercial kit (Biolabo SA, Maizy, France; cat. # LP80209). All samples were assessed in duplicate. The homeostasis model assessment of insulin resistance (HOMA-IR) index was calculated as described by Matthews *et al.* (1985) and normalized to the values obtained in control rats (CRs).

Relaxation of aortic segments

Rats were anaesthetized with ketamine (50 mg·kg^{-1}) and diazepam (4 mg·kg^{-1}) and killed by bleeding. The thoracic aorta was carefully excised, cleaned of surrounding fat and connective tissue and placed in a Petri dish with Krebs–Henseleit solution (KHS) at 4°C. Composition of KHS was (in mM): NaCl 119, KCl 4.6, $CaCl_2$ 1.5, $MgCl_2$ 1.2, $NaHCO_3$ 24.9, glucose 11, KH_2PO_4 1.2 and EDTA 0.027. Aortae were cut into 4–5 mm long cylindrical segments. For circular isometric tension recording, each vascular cylinder was set up in an organ bath containing KHS at 37°C continuously bubbled with 95% O_2/5% CO_2, which gave a pH of 7.4, according to a method described previously (Angulo *et al.*, 1996). Tension was continuously recorded in a data acquisition system (MP100A BIOPAC System, Santa Barbara, CA, USA). Aortic segments were contracted with noradrenaline (NA; 10–30 nM) and, when a stable plateau was reached, increasing concentrations of ACh (0.01–10 μM), insulin (0.01 nM to 1 μM) or sodium nitroprusside (SNP; 1 nM to 10 μM) were added and vasodilator responses were determined. For evaluation of the acute effects of experimental treatments on endothelial vasodilatation, treatments were randomly assigned to different segments from the same animal and the experiments were systematically performed in parallel for each series of experiments. Each vascular segment received only one of the treatments.

Determination of cGMP content in rat aorta

Rat aortic segments treated for 30 min with vehicle, FM19G11 (1 μM), L-NAME (100 μM) or FM19G11 plus L-NAME, were exposed for 5 min to 10 μM ACh, immediately frozen in liquid nitrogen and then stored at –80°C until extraction for cyclic nucleotide assay. Cyclic nucleotides were extracted by homogenization in 6% trichloroacetic acid, followed by ether (H_2O saturated) extraction and lyophilization. cGMP concentration was determined by ELISA, using a kit from Cayman Chemical Company (Ann Arbor, MI, USA; cat. # 581021) (Angulo *et al.*, 2010).

Vascular reactivity of rat mesenteric arteries

Second- to third-order branches of mesenteric arterial tree (lumen diameter 200–400 μm) were obtained from omentum

specimens and dissected by carefully removing the adhering fat tissue. Arterial ring segments (2 mm long) were subsequently mounted on microvascular wire myographs (J.P. Trading, Aarhus, Denmark) for circular isometric tension recordings, as described previously (Rodríguez-Mañas *et al.*, 2003). The vessels were allowed to equilibrate for 30 min in KHS continuously bubbled with 95% O_2/5% CO_2 mixture to maintain a pH of 7.4. The passive tension and internal circumference of vascular segments when relaxed *in situ* under a transmural pressure of 100 mmHg (L_{100}) were determined. The arteries were then set to an internal circumference equivalent to 90% of L_{100}, at which the force development is close to maximal (Mulvany and Halpern, 1977). Preparations were then exposed to 125 mM K^+ (KKHS, equimolar substitution of NaCl for KCl in KHS) and the contractile response was measured. After a stabilization period, rat arteries were contracted with 1–3 μM NA (80% of KKHS-induced contraction, approximately) and relaxation responses were evaluated by cumulative additions of ACh (1 nM to 10 μM) to the chambers. Experiments were run in parallel. Concentration–response curves to the agents in arterial segments from the same animal that previously received only vehicle (0.01% DMSO) were considered as controls for the evaluation of the effects of different treatments.

Western blot analysis

Total protein extracts were obtained by homogenization of aortic tissue with a MagNA laser electric homogenizer using T-PER extraction reagent (Pierce Biotechnology, Inc., Rockford, IL, USA) according to the manufacturer's recommendations, with the addition of 1× protease inhibitor cocktail and 1× phosphatase inhibitor cocktail (Roche Diagnostics, Indianapolis, IN, USA). Equal amounts of protein extracts (20 μg) were loaded onto a 10% SDS-polyacrylamide gel and resolved by standard SDS-PAGE. Proteins were electrophoretically transferred onto PVDF membranes. Membranes were blocked with 5% skimmed milk in PBS containing 0.1% Tween 20 (Sigma Chemical Co., St. Louis, MO, USA) for 60 min and tested overnight with specific antibodies at 1:500 dilution against eNOS, phospho-eNOS (Ser1177) (Abcam, Cambridge, UK; cat. # ab66127 and ab75639, respectively), HIF-1α, HIF-2α (Novus, Littleton, CO, USA; cat. # NB100-105 and NB-100–122, respectively), Akt, phospho-Akt (Ser^{473}) (Cell Signaling, Danvers, MA, USA; cat. # 2920S and 4060S, respectively) and at 1:5000 dilution against β-actin (Sigma, St. Louis, MO, USA; cat. # A1978), which was used as loading control. Subsequently, membranes were incubated with rabbit anti-mouse or goat anti-rabbit HRP-conjugated secondary antibody (1:5000) (Sigma). Blots were visualized by the ECL detection system (Amersham Biosciences, Piscataway, NJ, USA). Results were quantified by densitometry using QuantityOne/Chemi-Doc Software (Bio-Rad, Barcelona, Spain).

Immunofluorescence

Rat aortic segments were fixed in 4% paraformaldehyde and incorporated in paraffin blocks. Antigen retrieval was achieved by heating deparaffinized tissue sections (5 μm) in citrate buffer (pH 6). Following blockade with 5% BSA plus 0.3% Triton X-100 (Sigma Chemical Co.) in PBS for 1 h at 37°C, sections were incubated with antibodies against phospho-Akt (1:100 dilution) or against phospho-eNOS (1:200 dilution) overnight at 4°C. After washout in PBS plus 0.3% Triton X-100, the sections were incubated with a secondary Alexa Fluor 546-conjugated goat anti-rabbit antibody (dilution 1:250; Life Technologies, Alcobendas, Spain) and with DAPI (Life Technologies) to counterstain nuclei for 1 h at room temperature. Sections were mounted and viewed by fluorescence microscopy (Olympus BX51, Tokyo, Japan). Controls without primary antibodies showed no non-specific reactivity (data not shown). Images from each aortic specimen were captured and the total number of endothelial cells (ECs) as well as the number of those positive for phosphorylated-endothelial NOS (p-eNOS) and phosphorylated-Akt (p-Akt) were determined and the % of ECs positive for p-eNOS and p-Akt were calculated.

Human tissues

Human penile tissue biopsies were obtained from nine men with ED who gave informed consent at the time of penile prosthesis insertion. The patients had an average age of 59.0 ± 2.3 years (range 46–71). Five were hypertensive, three had dyslipidaemia, two had type 2 diabetes, two had obvious cardiovascular disease, one suffered from atrial fibrillation, one was obese and two had a smoking habit. The aetiology of ED was considered as vascular in all patients. Healthy cavernosal specimens were obtained from 10 organ donors without a history of ED or vascular risk factors at the time of organ extraction for transplantation (average age 48.7 ± 5.3 years, range 23–62). The study was approved by the Ethics Committee of Hospital Santo Antonio, Porto [081/10(059-DEFI/077-CES)], where the samples were collected. Tissues were maintained at 4–6°C in M-400 solution (composition in mM: mannitol, 230; KH_2PO_4, 15; $K_2HPO_4{\cdot}3H_2O$, 43; KCl, 15; $NaHCO_3$, 10) until used, which was between 16 and 24 h after extraction (Angulo *et al.*, 2002; 2010; González-Corrochano *et al.*, 2013).

Experiments with human penile resistance arteries

Small penile arteries – helicine arteries (lumen diameter 150–400 μm), which are the terminal branches of deep penile arteries – were dissected by carefully removing the adhering trabecular tissue. Then arterial ring segments (2 mm long) were mounted on microvascular wire myographs for circular isometric tension recordings, as described previously (González-Corrochano *et al.*, 2013). The arteries were then set to an internal circumference equivalent to 90% in the same way as that described earlier for rat mesenteric arteries. The preparations were then exposed to 125 mM K^+ (KKHS) and the contractile response was measured. The arteries were contracted with 1–3 μM NA (80% of KKHS-induced contraction, approximately), and the relaxation response was evaluated by cumulative additions of ACh to the chambers. After extensive washout and an equilibration period, FM19G11 (1 μM) or vehicle (0.01% DMSO) was added 30 min before contraction with NA for re-evaluating ACh-induced responses.

Experiments with human corpus cavernosum (HCC) tissue

Strips of corpus cavernosum tissue (3 × 3 × 7 mm) obtained from human penile tissue specimens were immersed in 8 mL

organ chambers containing KHS, maintained at 37°C and aerated with 5% CO_2/95% O_2, pH 7.4. Each tissue strip was incrementally stretched to optimal isometric tension, as determined by maximal contractile response to 1 μM phenylephrine (PE). The preparations were then exposed to KKHS and the contractile response was measured. After an equilibration period, tissues were contracted with 1–3 μM PE (80% of KKHS-induced contraction) and relaxation responses were evaluated by cumulative additions of ACh to the chambers. After extensive washout and equilibration period, FM19G11 (1 μM) or vehicle (0.01% DMSO) was added 30 min before contraction with PE for re-evaluating ACh-induced responses.

Drugs and materials

Nomenclature used for drugs and molecular targets conforms to BJP's Concise Guide to Pharmacology (Alexander *et al.*, 2013). Tween 20, Triton X-100, NA (arterenol), PE, ACh, SNP, N^G-nitro-L-arginine methyl ester (L-NAME), wortmannin and rapamycin were obtained from Sigma Chemical Co. Human insulin (Humulin®) was obtained from Lilly España (Alcobendas, Madrid, Spain). FM19G11 (3-[(2,4-dinitrobenzoyl) amino]-benzoic acid 2-(4-methylphenyl)-2-oxoethyl ester) was synthesized at Departamento de Química Orgánica, Centro de Investigación Príncipe Felipe, Valencia, Spain. For *in vitro* experiments, all drugs were dissolved in deionized water, except for FM19G11, wortmannin and rapamycin, which were dissolved at 10 mM concentration in DMSO. The subsequent dilutions were made in deionized water. Final DMSO concentration was 0.01% or lower.

Statistical analysis

Two-factor ANOVA was applied to analyse the effects of the treatments on the complete concentration–response curves. Expression data and cGMP values were compared by one-factor ANOVA followed by Student–Newmann–Keuls test. pD_2 was defined as the –log M of the concentration required to obtain 50% relaxation. E_{max} is the maximal relaxation response expressed as a percentage. pD_2 and E_{max} data given in the text were compared by Student's *t*-test except those involving more than two groups where one-factor ANOVA followed by Student–Newmann–Keuls test was used.

Results

Systemic administration of FM19G11 restores endothelium-dependent vasodilatation in IRRs

Fructose-fed rats developed insulin resistance, as confirmed by the significant increase in the HOMA-IR score (3.15 ± 0.44-fold increase; $P < 0.001$). The increase in HOMA-IR was reduced to 1.70 ± 0.42 after 7 days of i.p. administration of FM19G11 (10 mg·kg^{-1}·day^{-1}) ($P < 0.05$ vs. untreated fructose-fed rats). Aortic segments from vehicle-treated IRRs displayed a significantly diminished vasodilator response to ACh (10 nM to 10 μM) than segments from CRs. Administration of FM19G11 completely reversed the impairment in endothelial vasodilatation, as ACh-induced responses in aortic segments from IRR treated with FM19G11 were not significantly different from those obtained in aortae from CRs (Figure 1A). Vasodilatation induced by insulin (0.01 nM to 1 μM) in aorta was also blunted in IRR and treatment of IRR with FM19G11 restored insulin-induced vasodilator responses to the level of CRs (Figure 1B). Endothelium-independent vasodilatations induced by the NO donor, SNP (1 nM to 10 μM), were not altered by the presence of insulin resistance and were not modified by the treatment with FM19G11 [pD_2 8.22 ± 0.04, 8.31 ± 0.13 and 8.42 ± 0.04 for CR, IRR and IRR + FM19G11; not significant (n.s.)].

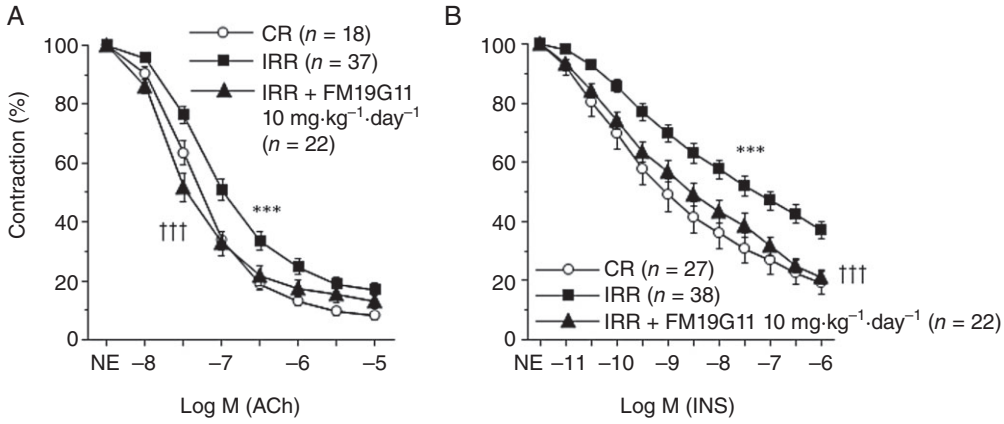

Figure 1

Recovery of endothelium-dependent vasodilatation in aorta from IRRs by chronic FM19G11. Effects of chronic administration of FM19G11 (10 mg·kg^{-1}·day^{-1}; i.p.) for 7 days on endothelium-dependent vasodilator responses to ACh (10 nM to 10 μM) (A) or insulin (0.01 nM to 1 μM) (B) in aorta from IRRs. Vasodilator responses obtained in aorta from CRs (non-insulin resistant rats) are shown for comparison. Data are expressed as mean ± SEM of the contraction induced by NA (1.80 ± 0.13, 1.88 ± 0.16 and 1.84 ± 0.1 g for CR, IRR and IRR + FM19G11 10 mg·kg^{-1}·day^{-1} in A, n.s.; 1.72 ± 0.17, 1.82 ± 0.08 and 1.86 ± 0.07 g for CR, IRR and IRR + FM19G11 10 mg·kg^{-1}·day^{-1} in B, n.s.). *n* indicates the number of vascular segments used for determinations that were obtained from 12 CRs, 16 IRRs and six IRRs treated with FM19G11. ***$P < 0.001$ versus CR and †††$P < 0.001$ versus IRR by a two-factor ANOVA test.

Acute pre-incubation of arteries from IRR with FM19G11 improves endothelium-dependent vasodilatation

Pre-incubation for 30 min with FM19G11 (1 μM) did not significantly modify endothelium-dependent relaxation of aortic segments from CR (Figure 2B). However, 0.3 μM FM19G11 moderately but significantly increased ACh-induced vasodilatation in IRR aorta (Figure 2C) and 1 μM FM19G11 markedly improved endothelial vasodilatation in IRR aorta (Figure 2A and D). At this latter concentration,

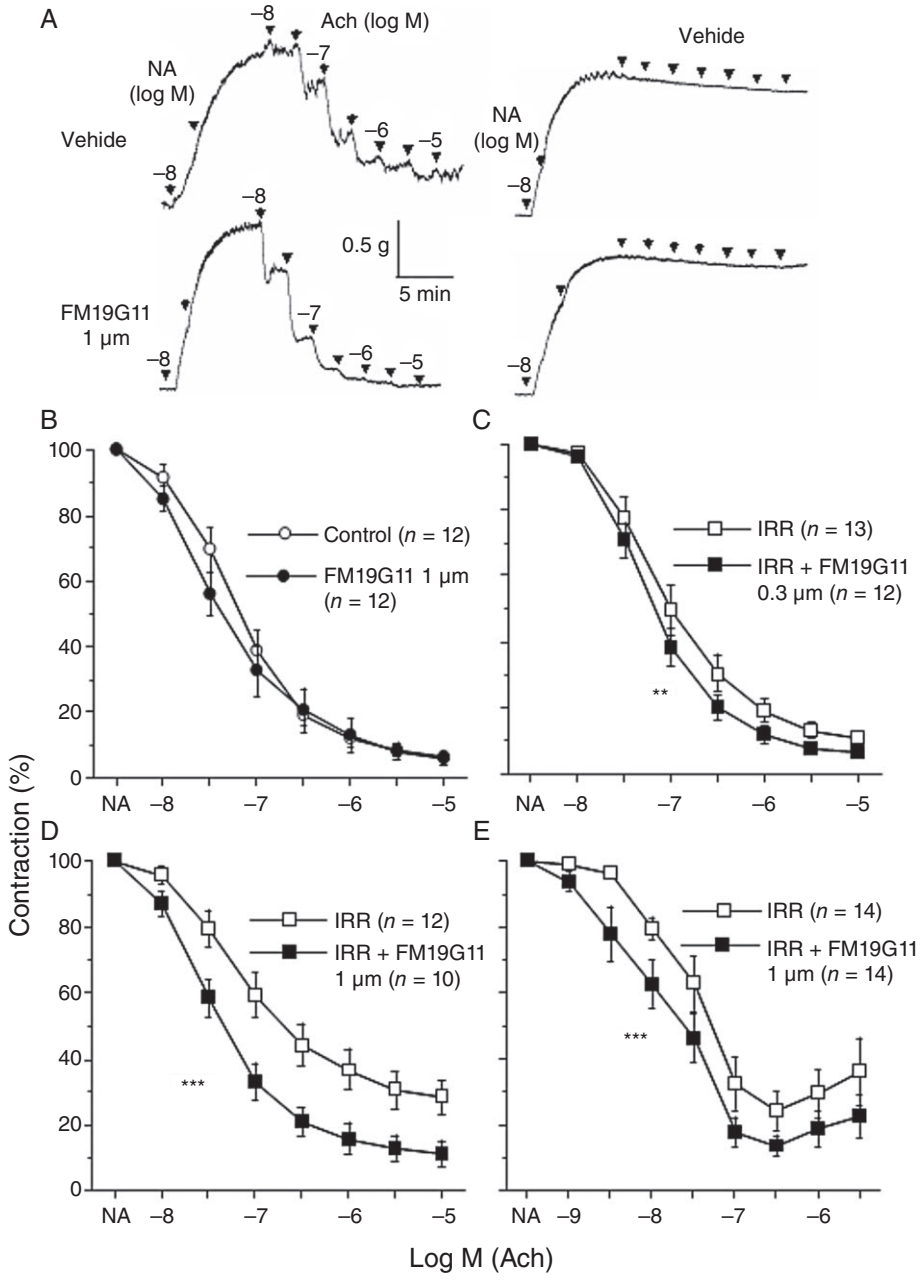

Figure 2

Acute treatment with FM19G11 improves endothelium-dependent vasodilatation in arteries from IRRs. Panel A displays representative tracings showing the improvement of endothelium-dependent vasodilator responses to ACh (10 nM to 10 μM) mediated by FM19G11 (1 μM) (left traces) and the lack of contractile tone destabilization by the same treatment (right traces) in aortic segments from IRRs. Other panels show the effects of pre-incubation with FM19G11 (0.3 or 1 μM) on vasodilator responses to ACh in aorta from CRs (B), in aorta from IRR (C, D) or in mesenteric arteries from IRR (E). Data are expressed as mean ± SEM of the contraction induced by NA (1.99 ± 0.08 vs. 1.96 ± 0.10 g; 1.92 ± 0.12 vs. 1.86 ± 0.14 g; 1.77 ± 0.08 vs. 1.82 ± 0.07 g; and 9.28 ± 0.71 vs. 8.48 ± 0.82 mN, control vs. FM19G11 for B, C, D and E, respectively; n.s. for all comparisons). *n* indicates the number of vascular segments used for determinations obtained from, at least, three different animals. $^{**}P < 0.01$, $^{***}P < 0.001$ versus control by a two-factor ANOVA test.

FM19G11 also enhanced vasodilatation induced by insulin in IRR aorta (E_{max} 54.1 ± 4.0 vs. 70.7 ± 5.3%, $P < 0.05$). This improvement in endothelium-dependent vasodilatation by FM19G11 (1 μM) was confirmed in small mesenteric arteries from IRR rats (Figure 2E). Similar to that observed in aorta, ACh-induced responses were not significantly modified by FM19G11 (1 μM) in mesenteric arteries from CR (pD_2 7.48 ± 0.10 vs. 7.73 ± 0.25; n.s.).

The enhancement in endothelial vasodilatation induced by FM19G11 is unlikely to be due to destabilization of adrenergic tone. This is supported by the fact that the treatment with FM19G11 did not influence the NA-induced tone in aorta from IRR when vehicle was administered instead of ACh whereas potentiation of ACh-induced vasodilatation was clearly observed (Figure 2A). In addition, contraction data provided in figure legends demonstrate that the contractile tone does not affect the enhancing effects of FM19G11 on vascular relaxation.

Enhancing effects of FM19G11 on endothelial function are mediated by the NO/cGMP pathway

ACh-induced relaxation of aortic segments in IRR is mainly mediated by NO, as inhibition of NOS with L-NAME (100 μM) almost abolished endothelium-dependent vasodilatation. When the NOS inhibitor was present, FM19G11 (1 μM) failed to exert its enhancing effect on ACh-induced responses (Figure 3A). After exposure of aortic tissue to ACh, the intracellular content of the second messenger of NO, cGMP, was reduced in IRR. In ACh-stimulated aortic tissue from IRR, FM19G11 significantly increased the cGMP

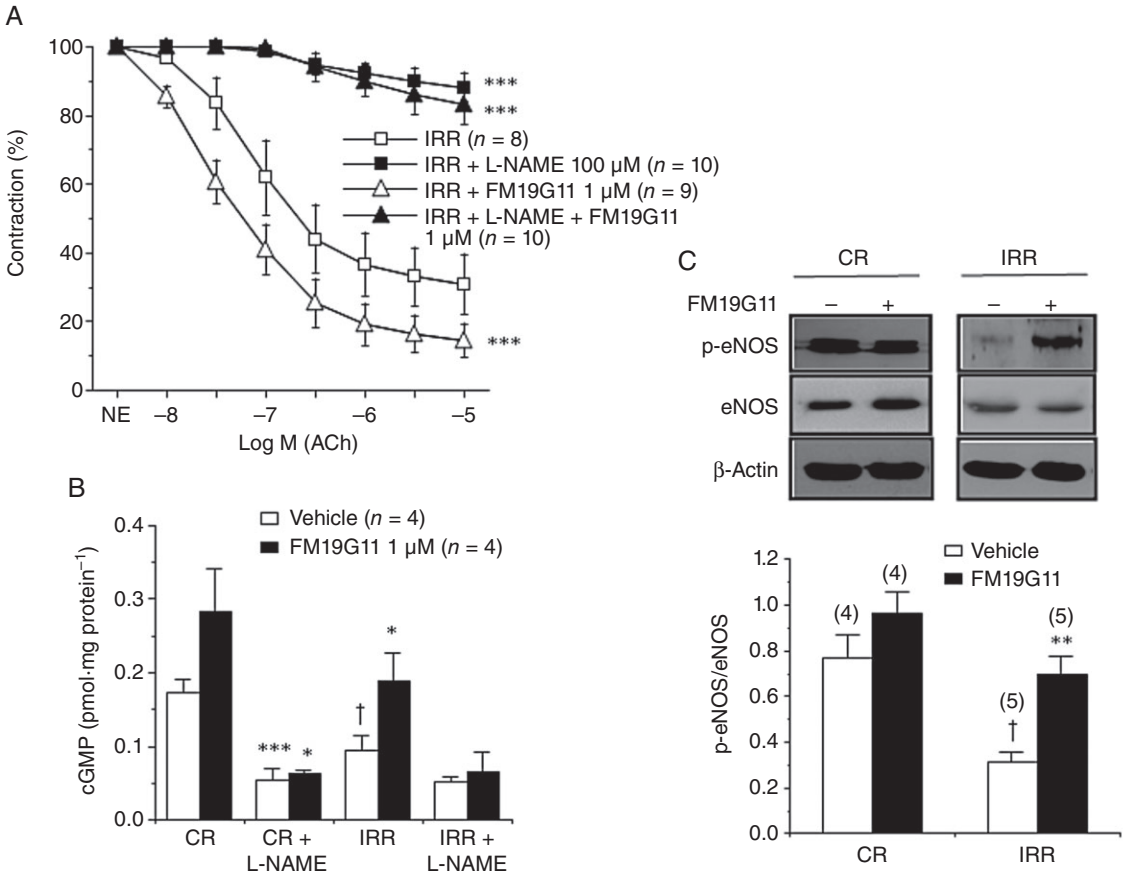

Figure 3

Involvement of the NO/cGMP pathway in FM19G11-induced improvement of endothelial vasodilatation in IRRs. Panel A shows the influence of the NOS inhibitor, L-NAME (100 μM), on the effects of FM19G11 (1 μM) on endothelium-dependent vasodilator responses to ACh (10 nM to 10 μM) in aorta from IRRs. Data are expressed as mean ± SEM of the contraction induced by NA (2.10 ± 0.33, 2.45 ± 0.32, 2.08 ± 0.23 and 2.44 ± 0.32 g for IRR, IRR + L-NAME, IRR + FM19G11 and IRR + L-NAME + FM19G11, respectively; n.s.). *n* indicates the number of vascular segments used for determinations obtained from, at least, three different animals. ***indicates $P < 0.001$ versus IRR by a two-factor ANOVA test. Panel B shows the effects of FM19G11 (1 μM) on cGMP accumulation induced by exposure to ACh (10 μM) in aortic tissue from CRs and IRR and the influence of L-NAME (100 μM) on such effects. *n* indicates the number of animals used for determinations. *indicates $P < 0.05$, ***$P < 0.001$ versus vehicle, and †$P < 0.05$ versus CR by a one-factor ANOVA followed by a Student–Newmann–Keuls test. Panel C shows the effects of FM19G11 (1 μM) on aortic content of eNOS and its phosphorylated (at Ser177) form (p-eNOS) in CR and IRR. Data are expressed as the normalized p-eNOS/eNOS ratio. Numbers of determinations appear in parentheses. **indicates $P < 0.01$ versus vehicle; †$P < 0.05$ versus CR by a one-factor ANOVA followed by a Student–Newmann–Keuls test.

content, while a non-significant increment was observed in aortic tissue from CR (Figure 3B). The requirement of NO synthesis for these effects on cGMP accumulation was confirmed by the fact that L-NAME reduced cGMP level in ACh-stimulated aortic tissue and prevented the increase in cGMP content induced by FM19G11 (Figure 3B). The amounts of the phosphorylated form of eNOS at Ser^{1177} (p-eNOS) relative to total eNOS content were significantly reduced in IRR aortae. Treatment with FM19G11 (1 μM) for 30 min caused a significant increase in the aortic p-eNOS/eNOS ratio in these rats (Figure 3C). FM19G11 (1 μM) did not significantly modify the total amount of eNOS in the aortae of CR or IRR (eNOS/β-actin ratios were 0.796 ± 0.118 and 0.805 ± 0.107 for vehicle- and FM19G11-treated aortae from CR, and 0.756 ± 0.135 and 0.732 ± 0.110 for vehicle- and FM19G11-treated aortae from IRR).

Improvement of endothelial vasodilatation in IRR aorta by FM19G11 involves activation of the PI3K/Akt/eNOS pathway

Inhibition of PI3K by wortmannin (500 nM) did not modify ACh-induced vasodilatation in IRR aorta significantly, but completely prevented the enhancement of these responses induced by FM19G11 (1 μM) (Figure 4A). This suggests that the PI3K/Akt pathway is involved in FM19G11-induced improvement in endothelial vasodilatation in IRR. In this context, although Akt expression was not significantly modified by FM19G11 (1 μM) (0.897 ± 0.170 and 0.863 ± 0.152 for vehicle- and FM19G11-treated aortae from IRR), an increased phosphorylation of Akt was observed after 30 min of incubation with FM19G11 (1 μM) in IRR aortae, an effect that was prevented by co-treatment with wortmannin (500 nM)

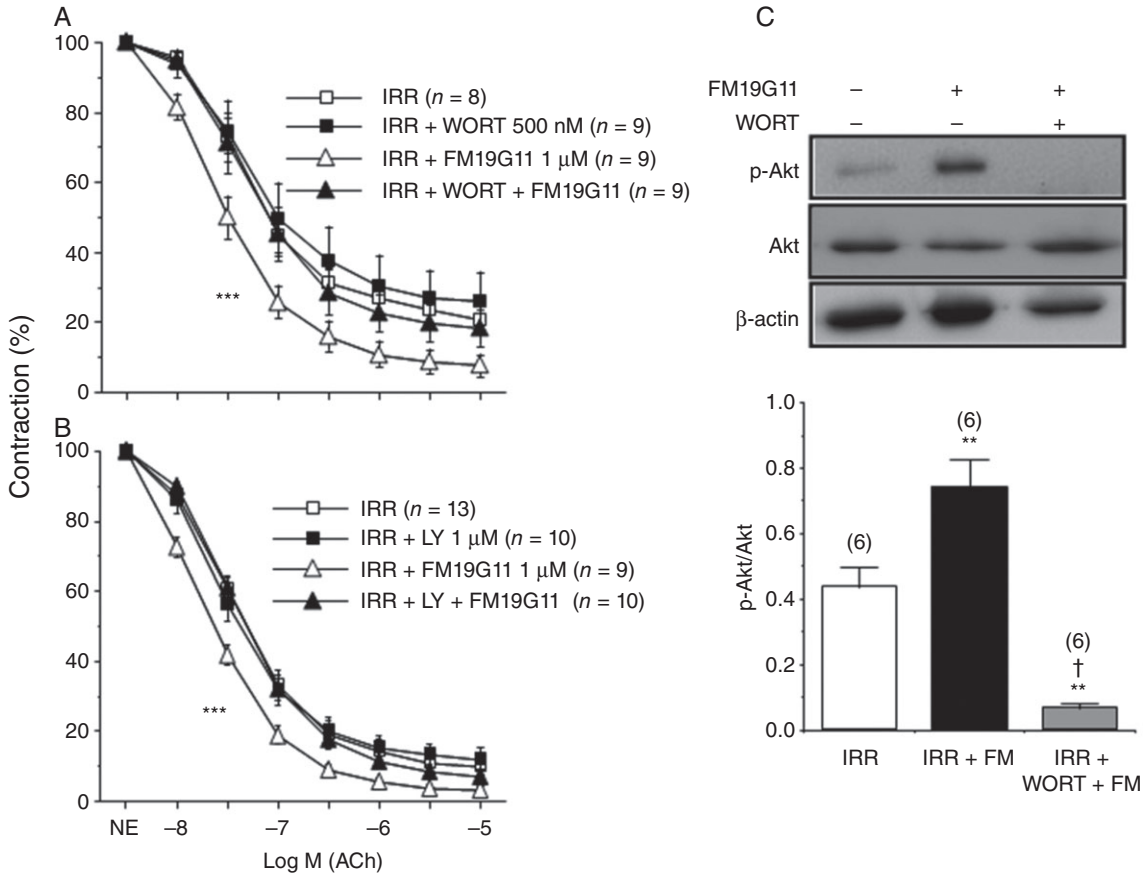

Figure 4

The PI3K/Akt pathway is involved in FM19G11-induced improvement of endothelial vasodilatation in IRRs. Influence of inhibition of PI3K with wortmannin (WORT; 500 nM) (A) or LY294002 (LY; 1 μM) (B) on the effects of FM19G11 (1 μM) on endothelium-dependent vasodilator responses to ACh (10 nM to 10 μM) in aorta from IRRs. Data are expressed as mean ± SEM of the residual contraction induced by NA (1.94 ± 0.14, 1.97 ± 0.14, 1.91 ± 0.17 and 2.02 ± 0.16 g for IRR, IRR + WORT, IRR + FM19G11 and IRR + WORT + FM19G11 in A; 1.64 ± 0.09, 1.82 ± 0.11, 1.66 ± 0.08 and 1.77 ± 0.14 g for IRR, IRR + LY, IRR + FM19G11 and IRR + WORT + FM19G11 in B; n.s. for all comparisons). *n* indicates the number of vascular segments used for determinations that were obtained from, at least, three different animals. ***$P < 0.001$, versus IRR by a two-factor ANOVA test. Panel C shows the effects of FM19G11 (1 μM) on aortic content of Akt and its phosphorylated (at Ser^{473}) form (p-Akt) in IRR and the influence of wortmannin on such effects. Data are expressed as the normalized p-Akt/Akt ratio. Numbers of determinations appear in parentheses. **$P < 0.01$ versus control and †$P < 0.05$ versus FM19G11 by a one-factor ANOVA followed by a Student–Newman–Keuls test.

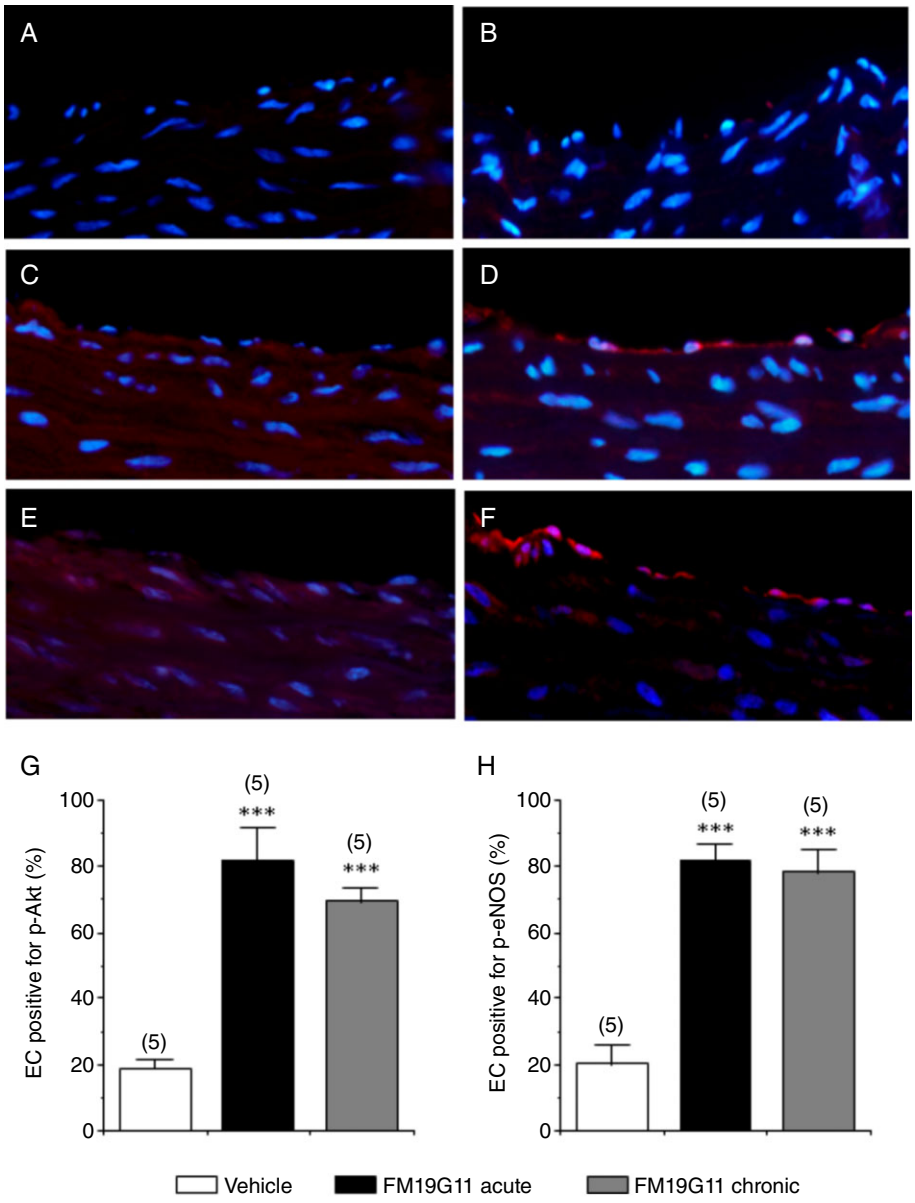

Figure 5

FM19G11 increases Akt/eNOS phosphorylation in aortic endothelium from IRRs. Immunodetection of phosphorylated forms of Akt (Ser^{473}) (left panels) and eNOS (Ser^{1177}) (right panels) in aortae from IRRs. Panels A and B show immunodetection in aortae from untreated IRR. In C and D, aortae from IRR were incubated for 30 min with 1 μM FM19G11. In E and F, aortae were obtained from IRR treated with FM19G11 (10 mg·kg^{-1}·day^{-1}; i.p.) for 7 days. Red fluorescence indicates positive signal. Lower panels show the mean ± SEM of the % of ECs positive for p-Akt (G) and p-eNOS (H) in aortae from IRRs after exposure to vehicle or FM19G11 either acute (*ex vivo*; 30 min with 1 μM FM19G11) or chronic (*in vivo*; 10 mg·kg^{-1}·day^{-1}; i.p. for 7 days). Numbers of determinations appear in parentheses. ***$P < 0.001$ versus IRR by one-factor ANOVA followed by Student–Newman–Keuls test.

(Figure 4B). Furthermore, increased amounts of the phosphorylated forms of Akt and eNOS were immunodetected in aortic endothelium from IRR after either chronic (7 days) or acute (30 min) exposure to FM19G11 (10 mg·kg^{-1}·day^{-1}; i.p. and 1 μM respectively) (Figure 5). Quantification of ECs positive for p-Akt in aortae from IRR yielded a significant increase in the % of ECs expressing p-Akt after acute or chronic exposure to FM19G11 (Figure 5G). Consistently, the % of ECs positive for p-eNOS increased in aorta from IRR after treatment with FM19G11 (Figure 5H).

Improvement of endothelial vasodilatation induced by FM19G11 is not dependent on an up-regulation of HIF-1α

Consistent with the previously reported ability of FM19G11 to up-regulate mTOR/HIF-1α signalling under normoxic con-

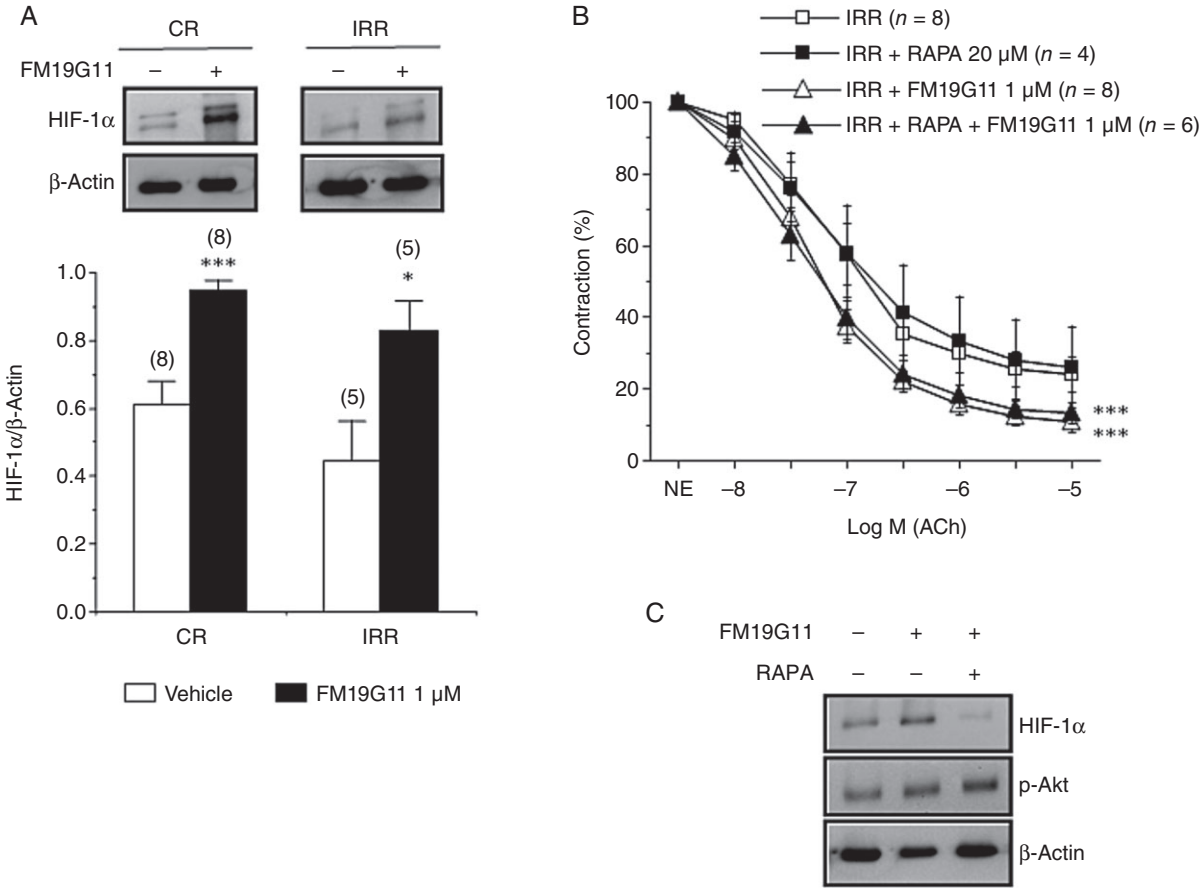

Figure 6

Up-regulation of HIF-1α by FM19G11 does not contribute to the improved endothelial vasodilatation in IRRs. Panel A shows the effects of FM19G11 (1 μM) on protein content of HIF-1α in aortic tissue from CR and IRRs. Data are expressed as the normalized HIF-1α/β-actin ratio. Numbers of determinations appear in parentheses. $*P < 0.05$, $***P < 0.001$ versus control by a one-factor ANOVA followed by a Student–Newmann–Keuls test. Panel B shows the influence of the mTOR inhibitor, rapamycin (RAPA; 20 μM), on the effects of FM19G11 (1 μM) on endothelium-dependent vasodilator responses to ACh (10 nM to 10 μM) in aorta from IRRs. Data are expressed as mean ± SEM of the contraction induced by NA. *n* indicates the number of vascular segments used for determinations that were obtained from, at least, three different animals. $***P < 0.001$ versus IRR by a two-factor ANOVA test. Panel C, representative blots showing that treatment with RAPA (20 μM) prevents FM19G11-induced HIF-1α up-regulation in aorta of IRR while it does not prevent FM19G11-induced Akt phosphorylation at Ser[473].

ditions in different cell types (Rodríguez-Jiménez *et al.*, 2012), treatment for 30 min with this compound resulted in increased aortic expression of HIF-1α protein in both CR and IRR (Figure 6A). However, this up-regulation of HIF-1α driven by FM19G11 does not seem to be responsible for the enhancing effects of FM19G11 on endothelial vasodilatation in IRR as the inhibition of mTOR with rapamycin (20 μM) did not prevent FM19G11-induced increased vasodilator responses to ACh in IRR aortae (Figure 6B). The Western blot depicted in Figure 6C clearly shows that mTOR inhibition by rapamycin (20 μM) prevented HIF-1α up-regulation induced by FM19G11 in aorta from IRR while it did not preclude FM19G11-induced enhancement of Akt phosphorylation. In contrast, the HIF-2α/β-actin ratio was not significantly modified by the treatment with FM19G11 (1 μM) in aortae from CR (0.877 ± 0.064 vs. 0.703 ± 0.187 for vehicle and FM19G11, respectively, $n = 3$) or IRR (0.706 ± 0.095 vs. 0.739 ± 0.175 for vehicle and FM19G11, respectively, $n = 3$).

FM19G11 reverses the impairment in endothelial vasodilatation of human penile arteries (HPRAs) and corpus cavernosum (HCC) from patients with vascular ED

Endothelium-dependent vasodilatation elicited by ACh (1 nM to 10 μM) in HPRA from patients with vascular ED was not modified after treatment with the vehicle (0.01% DMSO) (pD_2 5.93 ± 0.34 vs. 6.08 ± 0.32; n.s.). Impaired endothelial vasodilatation was observed in HPRA from ED patients when compared with HPRA from No ED subjects, but this impairment was reversed by treating arterial segments with FM19G11 (1 μM), as can be clearly observed from the tracings

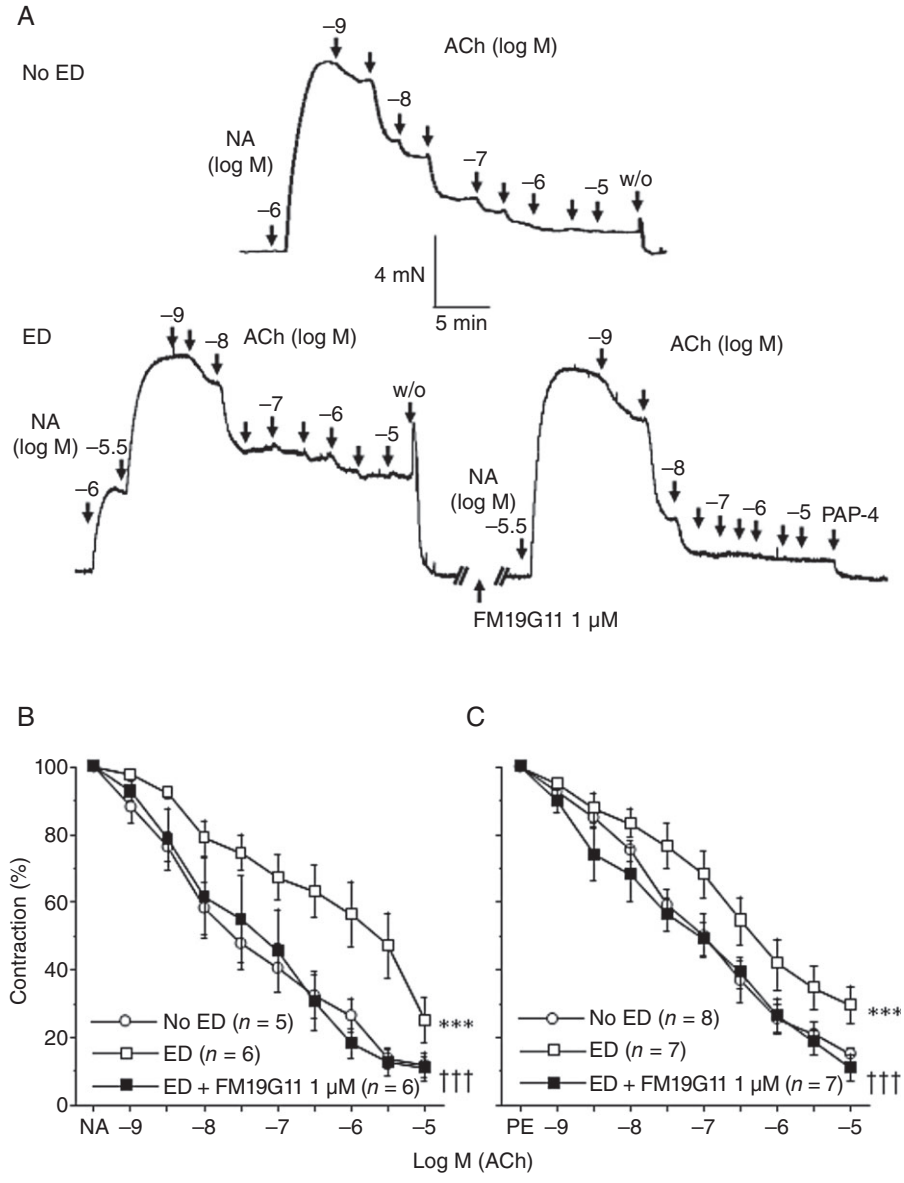

Figure 7

FM19G11 restores endothelium-dependent vasodilatation in human penile resistance arteries and corpus cavernsoum. Panel A shows representative tracings of the vasodilator responses to ACh (1 nM to 10 µM) in penile resistance arteries from a subject without known ED (No ED) (upper tracing) and from a patient with ED (lower tracings) before (left) and after (right) incubation with FM19G11 (1 µM) for 30 min. Other panels show the effects of FM19G11 (1 µM) on endothelium-dependent vasodilator responses to ACh in HPRAs (B) and HCC (C) from patients with ED. ACh-induced vasodilatation in HPRA and HCC from No ED subjects is shown for comparison. Data are expressed as mean ± SEM of the contraction induced by NA (6.73 ± 0.68, 6.26 ± 1.73 and 6.33 ± 1.51 mN for No ED, ED and ED + FM19G11, respectively; n.s. for all comparisons) and PE (1.20 ± 0.29, 0.99 ± 0.22 and 1.05 ± 0.20 g for No ED, ED and ED + FM19G11, respectively; n.s. for all comparisons), respectively. *n* indicates the number of patients from whom the tissues were collected. ***$P < 0.001$ versus No ED, †††$P < 0.001$ versus ED by a two-factor ANOVA test.

in Figure 7A. FM19G11 significantly potentiated the ACh-induced vasodilatation of HPRA (Figure 7B). This resulted in the recovery of endothelial vasodilatation in HPRA from patients with vasculogenic ED as endothelial vasodilator responses were comparable with those obtained in arteries from healthy penile tissues. Similar results were obtained when the effects of FM19G11 on endothelium-dependent relaxation of HCC were evaluated. FM19G11 (1 µM) improved relaxations induced by ACh (1 nM to 10 µM) in HCC from patients with vascular ED to a relaxation response similar to that obtained in HCC from patients without ED (Figure 7C).

Discussion

The present results show that chronic systemic administration of FM19G11 reverses the impairment of endothelium-

dependent vasodilatation induced by insulin resistance in rat aorta. In fact, short-term incubation with FM19G11 also improved endothelial vasodilatation in aorta and mesenteric arteries of IRRs. This effect of FM19G11 was (i) abolished by NO synthesis inhibition; (ii) prevented by PI3K inhibition; (iii) associated with an increment in the phosphorylated forms of Akt and eNOS, and an increase in cGMP in aortic tissue from IR rats. Hence, it is likely that the protective effect of FM19G11 is mediated through the PI3K/Akt/eNOS/cGMP pathway. Although the FM19G11-induced actions were paralleled by an increase in HIF-1α protein in aortic tissue, HIF-1α did not significantly contribute to the positive effects of FM19G11 on endothelial vasodilatation. The ability of FM19G11 to restore defective endothelium-dependent vasodilatation was confirmed in HPRAs and HCC from patients with endothelial dysfunction.

Ageing and metabolic disorders lead to an abnormal endothelial function that implies vascular damage and, ultimately, cardiovascular disease. Although there are portfolios of safe drugs to treat metabolic diseases, few of them, if any, are oriented to the endothelial function, with a view to avoiding the long-term undesired side effects of metabolic disorders, such as cardiovascular disease. Therefore, there is an urgent clinical need to identify novel mechanisms of action focusing on impeding endothelium deterioration. The rationale for evaluating the effects of FM19G11 on endothelial vasodilatation is based on evidence demonstrating its ability to activate PI3K/Akt and mTOR/HIF-1α in ependymal stem cells under normoxic conditions (Rodríguez-Jiménez *et al.*, 2012). The PI3K/Akt pathway regulates the phosphorylation of eNOS at Ser^{1177}, which results in increased synthesis of NO by this enzyme and enhances the vasodilatator response, a process that might be compromised in pathological conditions associated with endothelial dysfunction (Kobayashi *et al.*, 2004; Li *et al.*, 2010; Zhang *et al.*, 2012).

The results of the present study confirm the hypothesis that FM19G11 exerts positive effects on endothelial vasodilatation when endothelial dysfunction is present, as demonstrated by the data obtained after administration of the drug in a well-accepted rat insulin resistance model with endothelial dysfunction. The impairment of endothelial vasodilatation induced by insulin resistance in rats was reversed by chronic *in vivo* treatment with FM19G11. This beneficial *in vivo* effect on vasodilatation was also produced by short-term pre-incubation of the arteries *ex vivo*, suggesting that FM19G11 acts on vascular tissue. This effect was not limited to a specific vascular area as it occurred in both large (aorta) and resistance (mesenteric) arteries, which have different functions as regulators of blood flow. The improvement in vasodilatation induced by FM19G11 was mediated by the NO pathway in IRR aorta, as this effect was prevented by the NOS inhibitor, L-NAME. NO generation by the endothelium stimulates soluble GC in vascular smooth muscle, promoting cGMP formation, which triggers intracellular processes leading to smooth muscle relaxation and vasodilatation (Moro *et al.*, 1996). The accumulation of cGMP in aortic tissue in response to endothelial stimulation was reduced in IRR aorta, but was restored by exposure to FM19G11, demonstrating that this compound stimulates the NO/cGMP pathway. This is probably accomplished by the observed increase in eNOS phosphorylation induced by FM19G11 in aortic tissue from IRR. In fact, FM19G11 treatment restored the amount of phospho-eNOS in IRR aorta, which was lower than in CR. Therefore, phosphorylation at Ser^{1177} confers increased activity on eNOS, leading to augmented NO synthesis and enhanced vasodilatation. Thus, functional recovery of vasodilatation in IRR by systemic administration of FM19G11 could be triggered at the molecular level by an increased phosphorylation of eNOS. This result clearly suggests that pharmacological interventions leading to eNOS activation could be a reasonable way of overcoming endothelial dysfunction and thus preventing vascular damage.

Overactivation of PI3K/Akt is probably the mechanism leading to the increase in phospho-eNOS mediated by FM19G11, as inhibition of PI3K with wortmannin completely prevented the positive effects of FM19G11 on aortic vasodilatation in IRR. The involvement of PI3K/Akt in FM19G11-induced effects is further supported by the results obtained with an additional PI3K inhibitor, LY294002, which does not inhibit myosin light chain kinase at the concentration used (Yano *et al.*, 1995), but, similar to wortmannin, prevented the improvement of vasodilatation mediated by FM19G11 in aorta from IRR. In confirmation of these results, immunodetermination experiments showed that exposure to FM19G11 increased the phosphorylation of Akt in aortic tissue from IRR, and this effect was prevented by inhibition of PI3K. Although immunodetection of phosphorylated proteins, phospho-eNOS and phospho-Akt, in aortic tissue homogenates did not allow us to determine whether the endothelium or smooth muscle, which is the major component of aortic tissue, was the source of phosphorylated proteins, the results from the immunolocalization assays showed that both chronic and acute treatments with FM19G11 increased phospho-eNOS and phospho-Akt in aortic endothelium from IRR. This finding strongly suggests that FM19G11 activates the PI3K/Akt pathway in ECs, promoting increased phosphorylation and thereby activation of eNOS, the latter increasing NO availability and producing larger quantities of cGMP that cause enhanced vasodilatation. This concept is further supported by the ability of *in vivo* as well as *in vitro* treatment with FM19G11 to improve insulin-mediated vasodilatation, as this response is induced by eNOS phosphorylation via the PI3K/Akt pathway (Montagnani *et al.*, 2002; Kobayashi *et al.*, 2005; Gentile *et al.*, 2008). It is worth mentioning here that previous publications showed that FM19G11 also activates the serine/threonine-protein kinase ATR, a protein structurally related to PI3K (Rodríguez-Jiménez *et al.*, 2010; 2012).

FM19G11 has been shown to enhance glucose metabolism in ependymal stem cells (Rodríguez-Jiménez *et al.*, 2012). This is compatible with the lowering effect of FM19G11 on HOMA-IR in fructose-fed rats. In fact, because the action of insulin involves activation of PI3K/Akt signalling, the reduction in HOMA-IR would be consistent with the ability of FM19G11 to enhance this pathway. The reduction in HOMA-IR is an important feature that confers potential relevance to FM19G11 for increasing insulin sensitivity. However, although improved glucose clearance at the systemic level could contribute to the beneficial effects of chronic FM19G11 on endothelial function, it cannot explain the improving effect exerted by acute FM19G11, which is probably mediated by an effect on ECs.

It is important to note that FM19G11, in addition to activating the PI3K/Akt pathway, has also been reported to activate the mTOR/HIF-1α pathway and promote HIF-1α up-regulation in stem cells under normoxic conditions (Rodríguez-Jiménez *et al.*, 2010; 2012). This was also the case in rat vascular tissue as FM19G11 significantly increased the HIF-1α protein content of aortae from both CR and IRR. An up-regulation of HIF-1α has been shown to reverse the inability of aged mice to recover perfusion and motor function in ischaemic hindlimbs (Bosch-Marce *et al.*, 2007; Di *et al.*, 2013), restore the blunted inotropic response of hearts from old rats (Tan *et al.*, 2010) and contribute to cardiac repair induced by cell therapy (Cerrada *et al.*, 2013). Nevertheless, the elevation in HIF-1α triggered by FM19G11 does not seem to be associated with the ability of FM19G11 to overcome endothelial dysfunction in IRR. This was demonstrated by the finding that inhibition of mTOR by rapamycin prevented the increase in HIF-1α expression induced by FM19G11 but did not affect the increase in Akt phosphorylation and, consequently, did not impede the improvement of endothelial vasodilatation mediated by FM19G11 in IRR aorta. mTOR-mediated up-regulation of HIF-1α may be a consequence of PI3K/Akt pathway activation in normoxia (Agani and Jiang, 2013). Whether this is so for FM19G11 or it is produced by an independent mechanism is unrelated to the improvement of endothelial vasodilatation mediated by FM19G11, as reducing the expression of HIF-1α did not alter this effect of FM19G11. Although it has been suggested that HIF-2α is involved in endothelial homeostasis (Ahmad *et al.*, 2013) and it was reported that FM19G11 inhibited HIF-2α expression under hypoxic conditions in cancer cells and embryonic stem cells (Moreno-Manzano *et al.*, 2010), FM19G11 failed to significantly modify HIF-2α content in aortic tissue in our oxygen abundance conditions. HIF-2α expression is controlled by mTOR complex 2 (mTORC2) rather than mTORC1 (Toschi *et al.*, 2008). It is assumed that mTORC2 is less sensitive to rapamycin than mTORC1 but the high concentration of rapamycin (20 μM) used in our study has been demonstrated to block mTORC2 signalling in vascular tissue (Gao *et al.*, 2011). Thus, the lack of inhibition by rapamycin of FM19G11-induced improvement of endothelial vasodilatation in IRR suggests that any effects of FM19G11 on either HIF-1α or HIF-2α expression do not contribute to its ability to restore endothelial function.

Endothelial dysfunction associated with the presence of cardiovascular risk factors is assumed to play a key role in ED of vascular aetiology (Gratzke *et al.*, 2010). In fact, HPRA and HCC from patients with ED show an impaired endothelial vasodilatation, which is associated with a defective NO/cGMP pathway in penile tissue (Angulo *et al.*, 2010). The presence of a broad spectrum of cardiovascular risk factors, including elevated age, could contribute to endothelial dysfunction in our ED patients. In this context, treatment with FM19G11 improved endothelium-dependent vasodilatation in HPRA and HCC from patients with vascular ED, which may reflect the presence of systemic endothelial dysfunction (Gandaglia *et al.*, 2014). Thus, consistent with the results obtained in rats, FM19G11 is able to enhance endothelial vasodilatation in human vasculature characterized as having endothelial dysfunction and defective NO pathway. This demonstrates that the mechanism triggered by FM19G11 is effective at improving endothelial function in rat and human vasculature. It is not limited to the reversal of endothelial impairment specifically caused by insulin resistance, but seems to improve vasodilatation in a broader spectrum of pathological conditions associated with endothelial dysfunction.

In conclusion, FM19G11 improves endothelial dysfunction by an effect on the NO-mediated responses by a mechanism linked to activation of the PI3K/Akt pathway but not to mTOR activation/HIF-1α expression. This effect is not restricted to endothelial dysfunction associated with a specific pathological condition and seems to be present in both animal models of disease and human conditions.

Acknowledgements

We thank Argentina Fernández for her excellent technical assistance. This research work was supported by grants from the Ministerio de Economía y Competitividad (Instituto de Salud Carlos III, PI10/02781, PI11/01068, PI12/01628, S2010/BMD-2353, RETICEF RD12/0043), Spanish Government, and the Fundación Mutua Madrileña (AP103152012).

Author contributions

M. E. A., J. M. S.-P., L. R.-M. and J. A. were responsible for conception and design of the study. M. E. A., I. R., E. L.-H. and A. S.-F. acquired the data. J. L. A. synthesized FM19G11. M. E. A., J. M. S.-P., I. R., E. L.-H., A. S.-F., J. L. A., L. R.-M. and J. A. analysed and interpreted the data. M. E. A., J. M. S.-P. and J. A. drafted the manuscript. M. E. A., J. M. S.-P., I. R., E. L.-H., J. L. A., L. R.-M. and J. A. reviewed the manuscript for intellectual content. All authors revised and approved final version of the manuscript.

Conflict of interest

None of the authors have any conflict of interests.

References

Agani F, Jiang BH (2013). Oxygen-independent regulation of HIF-1: novel involvement of PI3K/AKT/mTOR pathway in cancer. Curr Cancer Drug Targets 13: 245–251.

Ahmad A, Ahmad S, Malcolm KC, Miller SM, Hendry-Hofer T, Schaack JB *et al.* (2013). Differential regulation of pulmonary vascular cell growth by hypoxia-inducible transcription factor-1α and hypoxia-inducible transcription factor-2α. Am J Respir Cell Mol Biol 49: 78–85.

Alexander SP, Benson HE, Faccenda E, Pawson AJ, Sharman JL, Spedding M *et al.* (2013). The concise guide to pharmacology 2013/14: Enzymes. Br J Pharmacol 170: 1797–1867.

Angulo J, Sánchez-Ferrer CF, Peiró C, Marín J, Rodríguez-Mañas L (1996). Impairment of endothelium-dependent relaxation by

increasing percentages of glycosylated human hemoglobin. Possible mechanisms involved. Hypertension 28: 583–592.

Angulo J, Cuevas P, La Fuente JM, Pomerol JM, Ruiz-Castañé E, Puigvert A *et al*. (2002). Regulation of human penile smooth muscle tone by prostanoid receptors. Br J Pharmacol 136: 23–30.

Angulo J, González-Corrochano R, Cuevas P, Fernández A, La Fuente JM, Rolo F *et al*. (2010). Diabetes exacerbates the functional deficiency of NO/cGMP pathway associated with erectile dysfunction in human corpus cavernosum and penile arteries. J Sex Med 7: 758–768.

Bosch-Marce M, Okuyama H, Wesley JB, Sarkar K, Kimura H, Liu YV *et al*. (2007). Effects of aging and hypoxia-inducible factor-1 activity on angiogenic cell mobilization and recovery of perfusion after limb ischemia. Circ Res 101: 1310–1318.

Cerrada I, Ruiz-Saurí A, Carrero R, Trigueros C, Dorronsoro A, Sánchez-Puelles JM *et al*. (2013). Hypoxia-inducible factor 1 alpha contributes to cardiac healing in mesenchymal stem cells mediated cardiac repair. Stem Cells Dev 22: 501–511.

Di Q, Cheng Z, Kim W, Liu Z, Song H, Li X *et al*. (2013). Impaired cross-activation of beta integrin and VEGFR-2 on endothelial progenitor cells with aging decreases angiogenesis in response to hypoxia. Int J Cardiol 168: 2167–2176.

Fisslthaler B, Dimmeler S, Hermann C, Busse R, Fleming I (2000). Phosphorylation and activation of the endothelial nitric oxide synthase by fluid shear stress. Acta Physiol Scand 168: 81–88.

Fujii N, Tsuchihashi K, Sasao H, Eguchi M, Miurakami H, Hase M *et al*. (2008). Insulin resistance functionally limits endothelium-dependent coronary vasodilation in nondiabetic patients. Heart Vessels 23: 9–15.

Gandaglia G, Briganti A, Jackson G, Kloner RA, Montorsi F, Montorsi P *et al*. (2014). A systematic review of the association between erectile dysfunction and cardiovascular disease. Eur Urol 65: 968–978.

Gao G, Li JJ, Li Y, Li D, Wang Y, Wang L *et al*. (2011). Rapamycin inhibits hydrogen peroxide-induced loss of vascular contractility. Am J Physiol Heart Circ Physiol 300: H1583–H1594.

Gentile MT, Vecchione C, Marino G, Aretini A, Di Pardo A, Antenucci G *et al*. (2008). Resistin impairs insulin-evoked vasodilation. Diabetes 57: 577–583.

Goksu C, Deveer M, Sivrioglu AK, Goksu P, Cucen B, Parlak S *et al*. (2014). Peripheral atherosclerosis in patients with arterial erectile dysfunction. Int J Impot Res 26: 55–60.

González-Corrochano R, La Fuente J, Cuevas P, Fernández A, Chen M, Sáenz de Tejada I *et al*. (2013). Ca^{2+}-activated K^+ channel (K_{Ca}) stimulation improves relaxant capacity of PDE5 inhibitors in human penile arteries and recovers the reduced efficacy of PDE5 inhibition in diabetic erectile dysfunction. Br J Pharmacol 169: 449–461.

Gratzke C, Angulo J, Chitaley K, Dai YT, Kim NN, Paick JS *et al*. (2010). Anatomy, physiology, and pathophysiology of erectile dysfunction. J Sex Med 7: 445–475.

Green DJ, Jones H, Thijssen D, Cable NT, Atkinson G (2011). Flow mediated dilation and cardiovascular event prediction. Does nitric oxide matter? Hypertension 57: 363–369.

Hanley AJ, Williams K, Stern MP, Haffner SM (2002). Homeostasis model assessment of insulin resistance in relation to the incidence of cardiovascular disease: the San Antonio Heart Study. Diabetes Care 25: 1177–1184.

Hisamoto K, Ohmichi M, Kurachi H, Hayakawa J, Kanda Y, Nishio Y *et al*. (2001). Estrogen induces the Akt-dependent activation of endothelial nitric-oxide synthase in vascular endothelial cells. J Biol Chem 276: 3459–3467.

Jackson G (2013). Erectile dysfunction and asymptomatic coronary artery disease: frequently detected by computed tomography coronary angiography but not by exercise electrocardiography. Int J Clin Pract 67: 1159–1162.

Katakam PV, Ujhelyi MR, Miller AW (1999). EDHF-mediated relaxation is impaired in fructose-fed rats. J Cardiovasc Pharmacol 34: 461–467.

Kilkenny C, Browne W, Cuthill IC, Emerson M, Altman DG (2010). Animal research: reporting *in vivo* experiments: the ARRIVE guidelines. Br J Pharmacol 160: 1577–1579.

Kobayashi T, Taguchi K, Yasuhiro T, Matsumoto T, Kamata K (2004). Impairment of PI3-K/Akt pathway underlies attenuated endothelial function in aorta of type 2 diabetic mouse model. Hypertension 44: 956–962.

Kobayashi T, Matsumoto T, Kamata K (2005). The PI3K/Akt pathway: roles related to alterations in vasomotor responses in diabetic models. J Smooth Muscle Res 41: 283–302.

Li R, Zhang H, Wang W, Wang X, Huang Y, Huang C *et al*. (2010). Vascular insulin resistance in prehypertensive rats: role of PI3-kinase/Akt/eNOS signaling. Eur J Pharmacol 628: 140–147.

Lteif AA, Han K, Mather KJ (2005). Obesity, insulin resistance, and the metabolic syndrome: determinants of endothelial dysfunction in whites and blacks. Circulation 112: 32–38.

Majmundar AJ, Wong WJ, Simon CS (2010). Hypoxia-inducible factors and the response to hypoxic stress. Mol Cell 40: 294–309.

Matthews DR, Hosker JP, Rudenski AS, Naylor BA, Treacher DF, Turner RC (1985). Homeostasis model assessment: insulin resistance and beta-cell function from fasting plasma glucose and insulin concentrations in man. Diabetologia 28: 412–419.

McGrath JC, Drummond GB, McLachlan EM, Kilkenny C, Wainwright CL (2010). Guidelines for reporting experiments involving animals: the ARRIVE guidelines. Br J Pharmacol 160: 1573–1576.

Michel T, Vanhoutte PM (2010). Cellular signaling and NO production. Pflugers Arch 459: 807–816.

Montagnani M, Ravichandran LV, Chen H, Esposito DL, Quon MJ (2002). Insulin receptor substrate-1 and phosphoinositide-dependent kinase-1 are required for insulin-stimulated production of nitric oxide in endothelial cells. Mol Endocrinol 16: 1931–1942.

Moreno-Manzano V, Rodríguez-Jiménez FJ, Aceña-Bonilla JL, Fustero-Lardíes S, Erceg S, Dopazo J *et al*. (2010). FM19G11, a new hypoxia-inducible factor (HIF) modulator, affects stem cell differentiation status. J Biol Chem 285: 1333–1342.

Moro MA, Russel RJ, Cellek S, Lizasoain I, Su Y, Darley-Usmar VM *et al*. (1996). cGMP mediates the vascular and platelet actions of nitric oxide: confirmation using an inhibitor of the soluble guanylyl cyclase. Proc Natl Acad Sci USA 93: 1480–1485.

Mulvany MJ, Halpern W (1977). Contractile properties of small resistance arteries in spontaneously hypertensive and normotensive rats. Circ Res 41: 19–26.

Paniagua OA, Bryant MB, Panza JA (2001). Role of endothelial nitric oxide in shear stress-induced vasodilation in human vasculature. Diminished activity in hypertensive and hypercholesterolemic patients. Circulation 103: 1752–1758.

Pawson AJ, Sharman JL, Benson HE, Faccenda E, Alexander SP, Buneman OP *et al*.; NC-IUPHAR (2014). The IUPHAR/BPS Guide to PHARMACOLOGY: an expert-driven knowledgebase of drug targets and their ligands. Nucl Acids Res 42 (Database Issue): D1098-D1106.

Reaven G (2012). Insulin resistance and coronary heart disease in nondiabetic individuals. Arterioscler Thromb Vasc Biol 32: 1754–1759.

Rodríguez-Jiménez FJ, Moreno-Manzano V, Mateos-Gregorio P, Royo I, Erceg S, Murguia JR *et al*. (2010). FM19G11: a new modulator of HIF that links mTOR activation with the DNA damage checkpoint pathways. Cell Cycle 9: 2803–2813.

Rodríguez-Jiménez FJ, Alastrue-Agudo A, Erceg S, Stojkovic M, Moreno-Manzano V (2012). FM19G11 favors spinal cord injury regeneration and stem cell self-renewal by mitochondrial uncoupling and glucose metabolism induction. Stem Cells 30: 2221–2233.

Rodríguez-Mañas L, Angulo J, Vallejo S, Peiró C, Sánchez-Ferrer A, Cercas E *et al*. (2003). Early and intermediate Amadori glycosylation adducts, oxidative stress, and endothelial dysfunction in the streptozotocin-induced diabetic rats vasculature. Diabetologia 46: 556–566.

Rodríguez-Mañas L, El-Assar M, Vallejo S, López-Dóriga P, Solís J, Petidier R *et al*. (2009). Endothelial dysfunction in aged humans is related with oxidative stress and vascular inflammation. Aging Cell 8: 226–238.

Royo I, Moreno-Manzano V, Rodríguez-Jimenez FJ, Sepúlveda P, Sánchez-Puelles JM (2011). The biology of HIFα proteins in cell differentiation and disease. Vitam Horm 87: 368–379.

Shinozaki K, Kashiwagi A, Nishio Y, Okamura T, Yoshida Y, Masada M *et al*. (1999). Abnormal biopterin metabolism is a major cause of impaired endothelium-dependent relaxation through nitric oxide/O_2-imbalance in insulin-resistant rat aorta. Diabetes 48: 2437–2445.

Suzuki M, Takamisawa I, Yoshimasa Y, Harano Y (2007). Association between insulin resistance and endothelial dysfunction in type 2 diabetes and the effects of pioglitazone. Diabetes Res Clin Pract 76: 12–17.

Symons JD, McMillin SL, Riehle C, Tanner J, Palionyte M, Hillas E *et al*. (2009). Contribution of insulin and Akt1 signaling to endothelial nitric oxide synthase in the regulation of endothelial function and blood pressure. Circ Res 104: 1085–1094.

Tan T, Marin-Garcia J, Damle S, Weiss HR (2010). Hypoxia-inducible factor-1 improves inotropic responses of cardiac myocytes in ageing heart without affecting mitochondrial activity. Exp Physiol 95: 712–722.

Thacker EL, Psaty BM, McKnight B, Heckbert SR, Longstreth WT Jr, Mukamal KJ *et al*. (2011). Fasting and post-glucose load measures of insulin resistance and risk of ischemic stroke in older adults. Stroke 42: 3347–3351.

Toschi A, Lee E, Gadir N, Ohh M, Foster DA (2008). Differential dependence of hypoxia-inducible factors 1α and 2α on mTORC1 and mTORC2. J Biol Chem 283: 34495–34499.

Tran LT, Yuen VG, McNeill JH (2009). The fructose-fed rat: a review on the mechanisms of fructose-induced insulin resistance and hypertension. Mol Cell Biochem 332: 145–159.

Yano H, Agatsuma T, Nakanishi S, Saitoh Y, Fukui Y, Nonomura Y *et al*. (1995). Biochemical and pharmacological studies with KT7692 and LY294002 on the role of phosphatidylinositol 3-kinase in FcεRI-mediated signal transduction. Biochem J 312: 145–150.

Zhang QJ, Holland WL, Wilson L, Tanner JM, Kearns D, Cahoon JM *et al*. (2012). Ceramide mediates vascular dysfunction in diet-induced obesity by PP2A-mediated dephosphorylation of the eNOS-Akt complex. Diabetes 61: 1848–1859.